Journal of Innovative Optical Health Sciences
Vol. 13, No. 1 (2020) 2050003 (10 pages)

DOI: 10.1142/S1793545820500030

Investigation of optical reflectance from different animal vertebra along the fixation trajectory of pedicle screw in frequency domain

Yangyang Liu*,†, Huan Zhang*, Ying Tong†, Zhiyu Qian* and Weitao Li*,‡
*Department of Biomedical Engineering
Nanjing University of Aeronautics and Astronautics
Nanjing, Jiangsu, P. R. China
†College of Information and Communication Engineering
Nanjing Institute of Technology
Nanjing, Jiangsu, P. R. China
‡liweitao@nuaa.edu.cn

Received 22 September 2019
Accepted 7 November 2019
Published 11 December 2019

Accurate placement of pedicle screw (PS) is crucial in spinal surgery. Developing new real-time intra-operative monitoring and navigation methods is an important direction of clinical application research. In this paper, we studied the spectrum along the fixation trajectory of PS in frequency domain to tackle the accuracy problem. Fresh porcine vertebrae, bovine vertebrae and ovine vertebrae were measured with the near-infrared spectrum (NIR) device to obtain the reflected spectrum from the vertebrae. Along the fixation trajectory of PS, average energy from different groups was calculated and used for identifying different tissues and compared to achieve the optimal recognition factor. Compared with the time domain approach, the frequency domain method could divide the spectra measured at different tissue points into different groups more stably and accurately, which could serve as a new method to assist the PS insertion. The results gained from this study are significant to the development of hi-tech medical instruments with independent intellectual property rights.

Keywords: Pedicle screw fixation; frequency domain; optical reflectance; vertebra.

1. Introduction

Pedicle screw (PS) internal fixation has been commonly used for correcting instability of spine. Accuracy in placement of PS is very important for an effective PS fixation.[1–4] Nowadays, the clinical standard for evaluation of PS position is by using

‡Corresponding author.

postoperative computed tomography (CT) scan.[5,6] However, this method is not applicable as a real-time monitoring method during surgery. The X-ray fluoroscopy can be used in real time, but the limitation is that the radiation dose to surgeons is high and scans must be done several times.[7,8] The electrical conductivity measuring device was introduced, which enables real-time detection of independent parameters of different tissues.[9] However, it is inevitable that the sensitivity of electrical conductivity of tissue is very low. Thus, accurate and reliable insertion of PS remains a challenge.

In previous research, we have presented the design and implementation of the fiber optic free-hand drilling probe and the spectrum measurement system for *in vitro* assessment of pattern from the optical reflectance.[10,11] Based on this device, we have found some ways in time domain to explore the different tissues of porcine vertebra along the fixation trajectory of PS by comparing the specific peak and the slope value of the reflected spectrum. However, these methods have some disadvantages, which cannot be avoided. For example, the classification accuracy of these methods is easily affected by the instrument.

In this study, we first collected and compared the optical reflectance spectra from three different animal models along the fixation trajectory, including fresh porcine vertebrae, bovine vertebrae and ovine vertebrae. These models were chosen because porcine vertebra was similar to that of human, and bovine and ovine vertebrae were similar in composition, used as vertebral models in some research.[12] Our goal was to develop a different method to analyze the characteristic of the corresponding spectrum and distinguish tissues according to the different characteristics.[13–15] Along the fixation trajectory of pedicle screw, average energy patterns used for identifying different tissues were calculated in frequency domain.[16,17]

Specifically, the spectra from different animal vertebral bones at similar positions along the trajectory were investigated simultaneously. The same vertebra tissues had similar reflectance spectra among different animal species. In frequency domain, FFT changes of spectra during specific band were conducted and the energies of specific band were analyzed, named F_{energy}. Finally, F_{energy} factor and slope factor in time domain[11] were compared from different aspects such as sensitivity, accuracy and correlation. It was found that the frequency domain method could divide the spectrums of different tissue measurement points into different groups more stably and accurately. To our knowledge, this is the first study of simple, accurate, and sensitive method to monitor the PS during fixation based on optical reflectance spectrum collected by the spectrum measurement system. The methods presented in this study could serve as a new approach to assist PS insertion.

2. Materials and Methods

2.1. *Instrument*

The experimental set-up for spectrum measurement is shown in Fig. 1. The system consists of a tungsten halogen light source (HL2000-HP-FHSA, Ocean Optics, Inc., Dunedin, FL), fiber optic probe, spectrometer (USB2000, Ocean Optics, Inc., Dunedin, FL) and a computer.[10,11] The home-made stainless-steel bifurcated fiber optic free-hand drill probe holder contains two 200-μm diameter fibers for light delivery and collection, respectively, with an outer diameter of 5 mm. The controller is used to adjust the light intensity. Data acquisition, scan conversion and display were implemented in real time at 2 frames per second in commercial LabView interface software (National Instrument, Austin, TX). The optical reflectance spectra were analyzed using custom made software in LabView and Matlab (The Math Works, Natick, MA).

2.2. *Vertebral bones experiment*

The human vertebra was similar to that of porcine, especially between T6 and T10.[18,19] We chose these

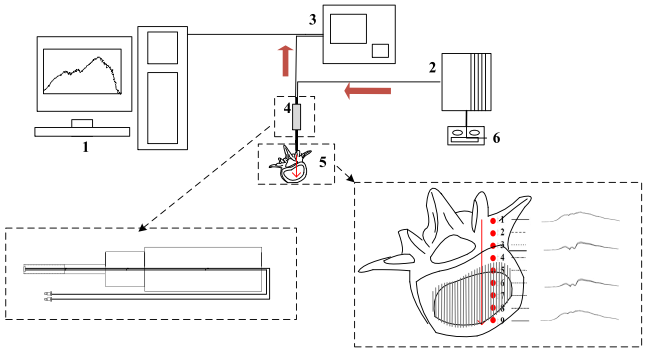

Fig. 1. The measurement system for spectrum on the vertebral bone model: 1: computer, 2: light source, 3: spectrometer, 4: fiber optic probe, 5: vertebral bone model, 6: controller.

porcine vertebrae in the experiment. The study comprised 10 fresh vertebral bones, which were taken from mature pig cadavers weighting 38–45 kg. All vertebral bones carefully cleaned off all soft tissues, except the periosteum. First, the puncture path (nine points) in the vertebra was planned as shown in the red arrow line (Fig. 1). Normally, the length of the trajectory varies between 22 mm to 35 mm. The distance between each of the two sampling points was about 5 mm. Then, the optic probe was drilled into vertebra to measure each sampling point. According to the scale on the handle, the probe was drilled 5 mm into the vertebra every time. In order to eliminate the volatility, 30 spectra were recorded and stored for each point. Integration time was 100 ms and the optical reflectance spectra consisted of 2048 pixels.

During the bovine vertebra experiment, 10 fresh vertebral bones were extracted from mature cow cadavers weighting 300–350 kg. The light spectra were produced in a two-step process, similar to the steps in porcine vertebra experiment. Nine sampling points were chosen with an 8 mm distance between each of the two sampling points, due to the larger size of cow vertebral bone. Ovine vertebra experiment also comprised 10 fresh vertebral bones, which were used from mature sheep cadavers weighting 70–80 kg. The size of sheep vertebra is smaller than those of pig or cow vertebra. Therefore, the sampling points have the smallest distance between each other. Other experimental steps are similar to those in porcine vertebra experiments.

Statistical analysis was performed with the Student t-test. A 95% confidence level was chosen to determine the significance of differences between groups, with a P value of less than 0.05 indicating a significant difference.

2.3. *Recognition factor in frequency domain*

The optical reflectance spectra consisted of 1024 CCD pixels and were imported into MATLAB for processing using in-house written software codes. Then, F_{energy} was calculated from original spectrum by frequency domain approach. If the spectra were looked as common curve with intensity via wavelength (nm), fast fourier transform (FFT) could be used to analyze the change cycles per nm. The information in frequency domain is more stable than that in time domain in this case. The point number of FFT is named N and the wavelength range is from A to B. Then, it defined the sampling frequency in wavelength as F_s, shown as Eq. (1).

$$F_s = \frac{N-1}{B-A}. \tag{1}$$

In this paper, N is 2048. Wavelength range is from 339.99 nm to 1019.64 nm. Then, $F_s = 3.012$ (1/nm). The sampling interval in horizontal coordinate was $F_s/(N-1) = 0.00147$ (1/nm). Because there were different numbers of each band, we calculated the average energy of some points and compared. Then, it was differences between two different vertebra tissues were found. Specifically, in order to search for the optimal recognition factor, FFT changes of different bands were done and average energy of different frequency sections were compared after FFT changes. F_{energy} was defined as the average amplitude value of points during specific frequency section after FFT changes of specific band.

3. Experimental Results

3.1. *Original spectrum*

Figure 2 shows a representative initial spectrum relating to the nine sampling points along the trajectory from one vertebra of each of the three animal species. Each spectrum curve represents the value in one sampling point on one animal vertebra. Points 1 and 9 are in the cortical bones and points 2 to 8 are in the cancellous bones. In Fig. 2, the values of points 1 and 9 in cortical bones are distinct from those in the cancellous bones. In Fig. 2(a), the values of points 1 and 9 are larger than those of points 2 to 8. However, the values of points 1 and 9 are smaller than those of points 2 to 8 in some bands in Figs. 2(b) and 3(c).

3.2. *Optimal recognition factor*

The initial curves can be analyzed in frequency domain by FFT. FFT changes over the whole band (339.99 nm to 1019.64 nm) were shown in Fig. 3. The amplitude differences of different tissues were obvious but it is not easy to extract. In Fig. 2, it is found that the differences in spectra between cortical bones and cancellous bones exist in the entire band, especially remarkable from 450 nm to 750 nm. Therefore, FFT changes were mainly analyzed within this specific band.

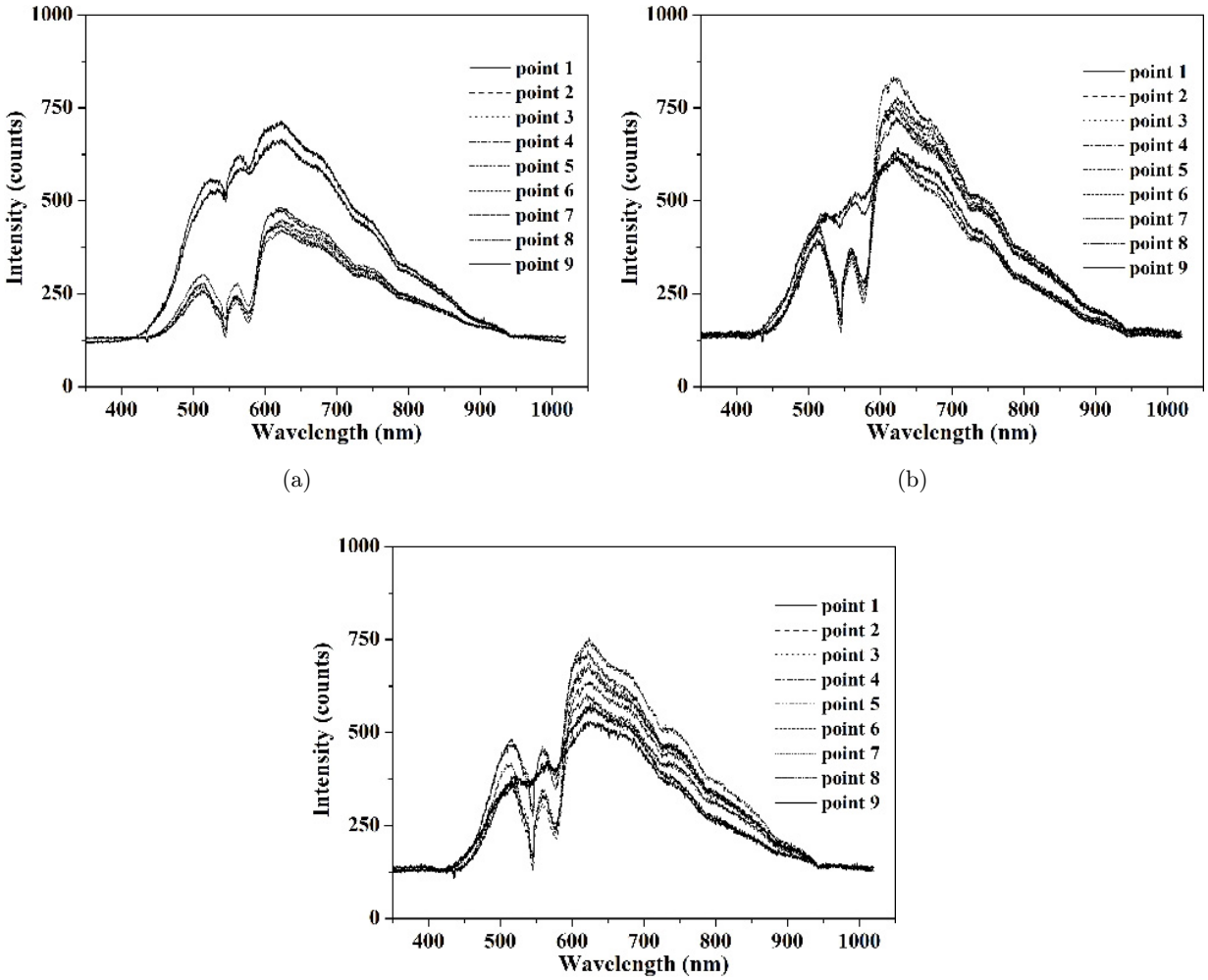

Fig. 2. Original spectra of different animal vertebra (a) porcine vertebra, (b) bovine vertebra, (c) ovine vertebra.

The value of amplitude was summed and averaged over cortical bones and cancellous bones, respectively. The proposed patterns were compared between the two different tissues using the calculated average amplitude values. Specifically, we chose different band groups to calculate average energy such as 450 nm to 500 nm. The total number of all the groups is 21. Then, the sample points were divided into two groups based on cortical bones and cancellous bones and mean amplitude values from each group was calculated. The average amplitude value from different band groups in porcine vertebra experiment is shown in Fig. 4(a). Then, we calculated the differences between two different vertebra tissues and the results are shown in Fig. 4(b). Here, the calculated differences were defined as $D = (V_{\text{cortical bone}} - V_{\text{cancellous bone}})/V_{\text{cortical bone}}$. The results show that the average amplitude value (550 nm to 750 nm) has the largest absolute value among all the bands.

In order to explore further, FFT changes of 550 nm to 750 nm were done as a foundation and average energy of different frequency section were compared after FFT changes. Figure 4(c) shows average energy values after FFT changes in porcine vertebra experiment based on two groups (cortical bone group and cancellous bone group). Then, we calculated the differences (with the same method abovementioned) between two different vertebra tissues in Fig. 4(d). The results show that the difference of average energy (4 Hz to 5 Hz) has the largest absolute value, which could be used as a characteristic factor (F_{energy}) to distinguish between the two tissues.

We conducted the same analysis with bovine vertebra experiment and ovine vertebra experiment.

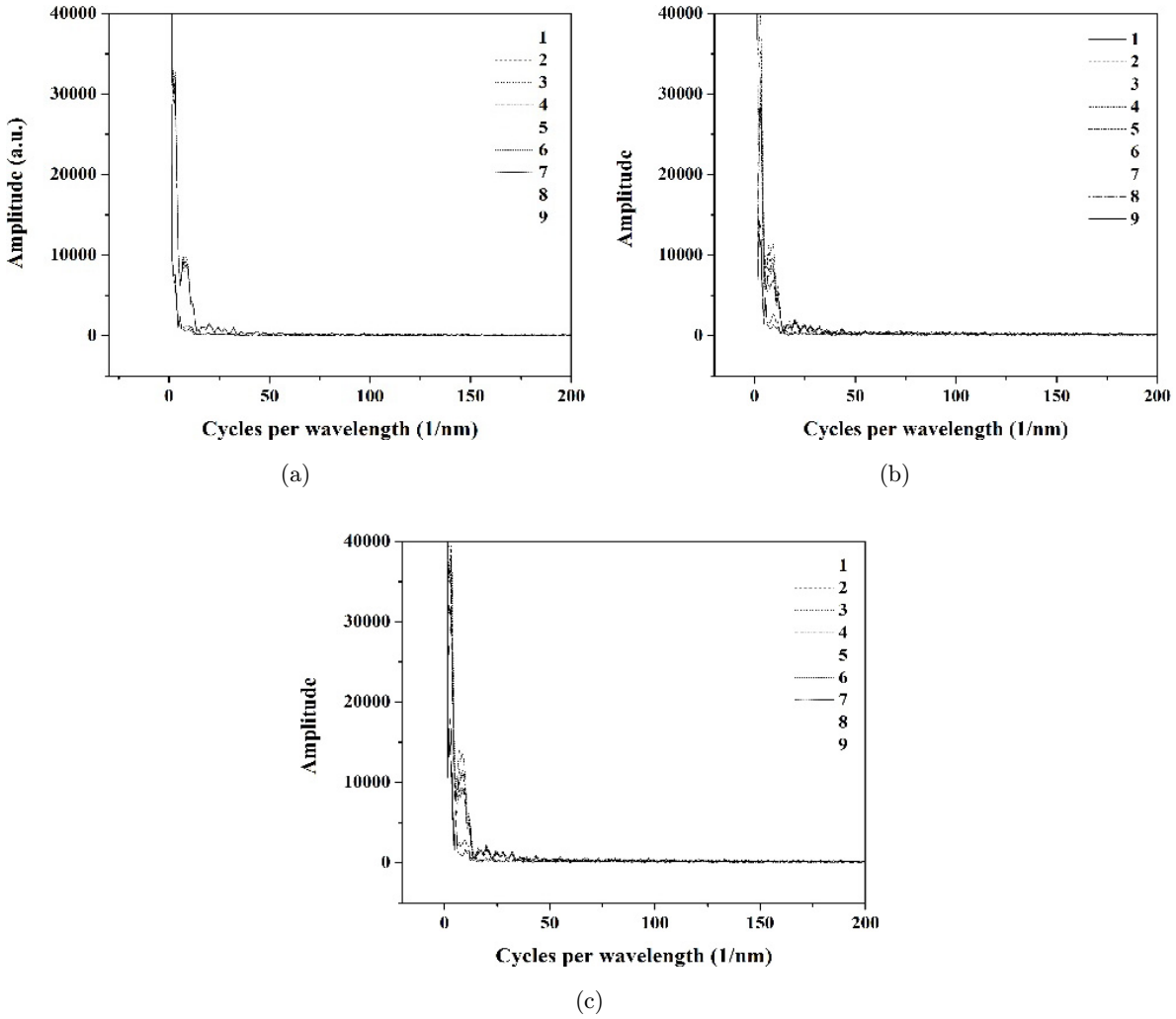

Fig. 3. FFT changes over the whole band in different animal vertebra experiment (a) porcine vertebra, (b) bovine vertebra, (c) ovine vertebra.

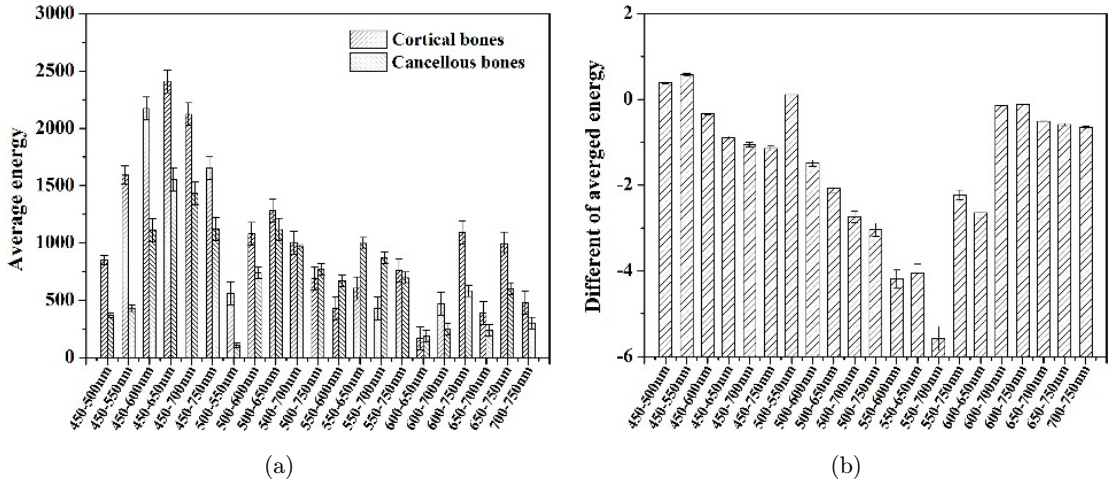

Fig. 4. Average energy from different groups based on the two tissues with porcine vertebra experiment (a) the average energy from different band groups, (b) the difference of average energy from different band groups, (c) the average energy from different frequency section (550 nm to 750 nm), (d) the difference of average energy from different frequency section (550 nm to 750 nm).

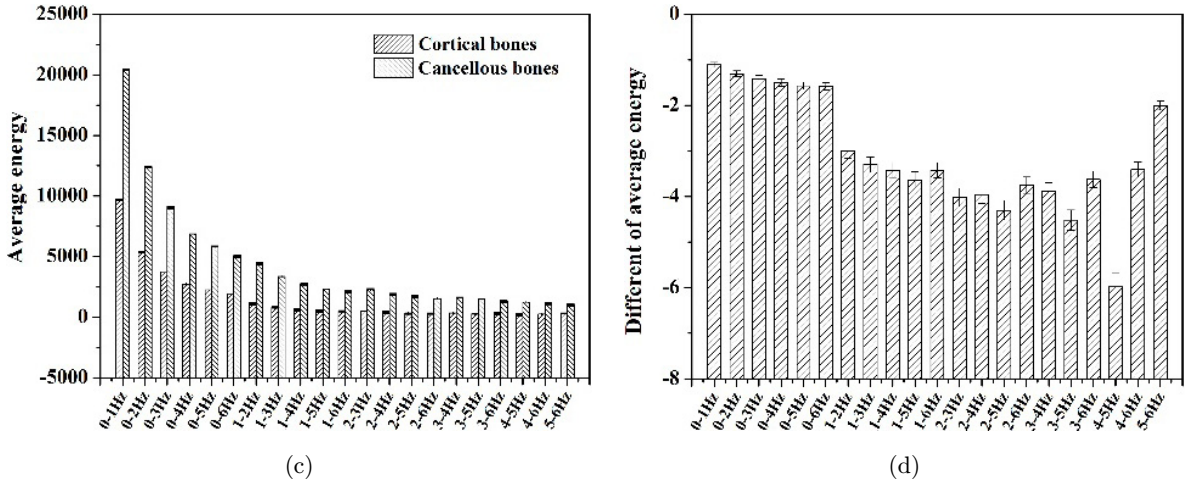

(c) (d)

Fig. 4. (*Continued*)

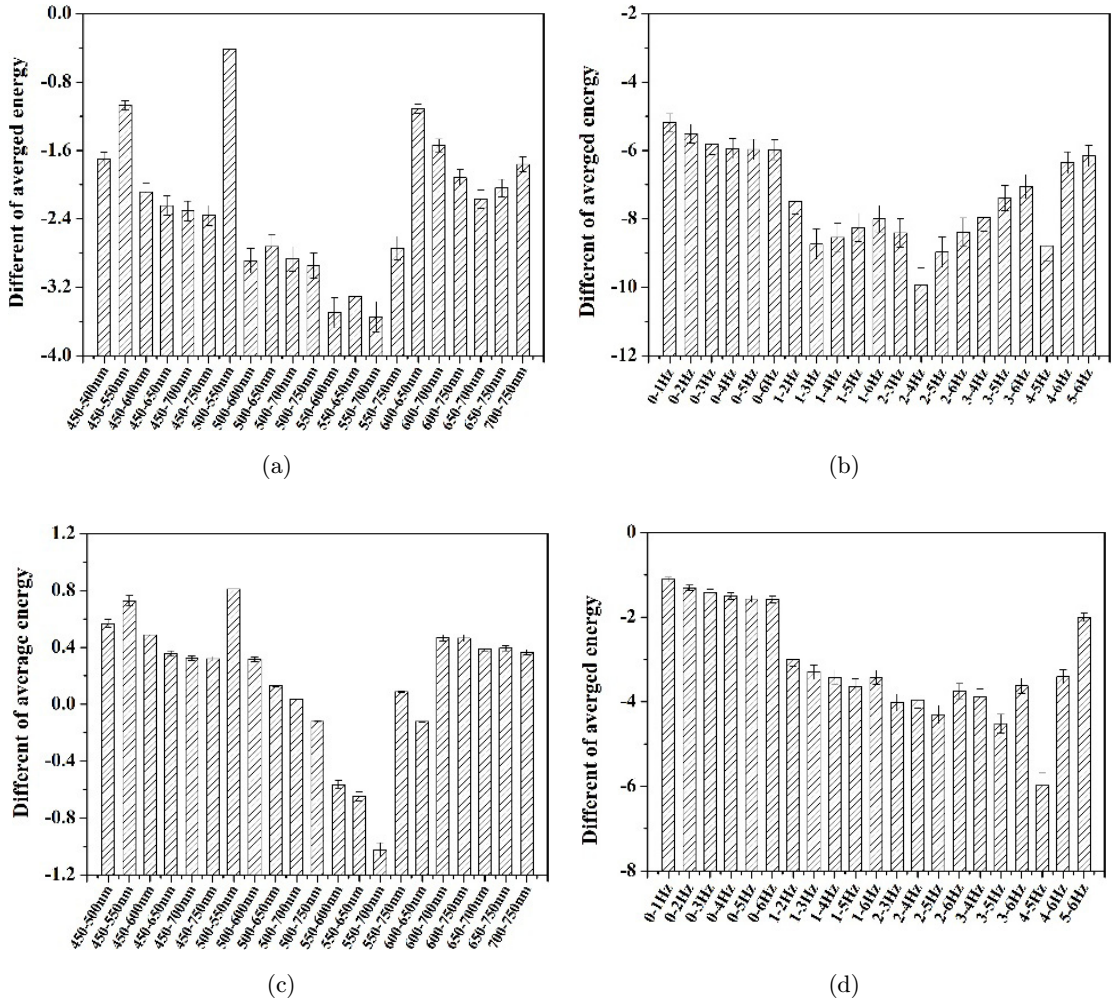

(a) (b)

(c) (d)

Fig. 5. Differences of average energy from different band groups in cow and sheep vertebra experiment. (a) different band groups in cow vertebra experiment, (b) different frequency section after FFT changes in cow vertebra experiment (550 nm to 750 nm), (c) different band groups in sheep vertebra experiment, (d) different frequency section after FFT changes in sheep vertebra experiment (550 nm to 750 nm).

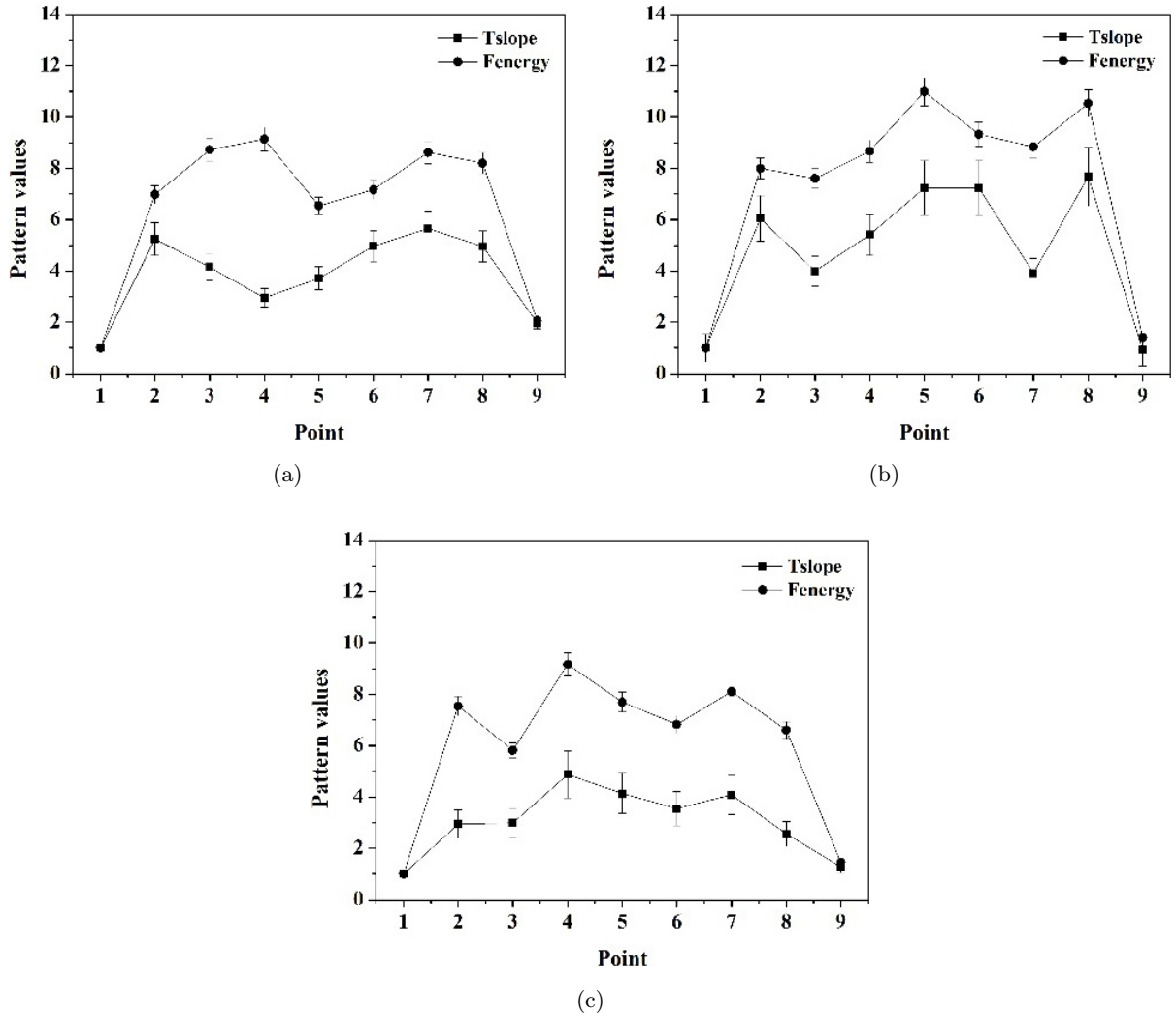

Fig. 6. The pattern values of nine sample points from different animal vertebra models. (a) porcine vertebra models, (b) bovine vertebra models, (c) ovine vertebra models.

The related results for bovine vertebra were shown in Figs. 5(a) and 5(b). The results for ovine vertebra were shown in Figs. 5(c) and 5(d). These results were similar to those of the pig vertebra.

3.3. *Compare different patterns*

In addition, we calculated F_{energy} in frequency domain and slope factor in time domain (named T_{slope}) and compared the two. Based on the previous studies, T_{slope} (500–550 nm) from the original light spectra could be used to express the difference between the two tissues of porcine vertebrae.[19] The average values of T_{slope} of nine sample points after normalization from porcine vertebra models are shown in Fig. 6(a). The result showed that the absolute slope values of the curve at both ends are larger and T_{slope} has a high distinguishable ability. However, the average F_{energy} values of each sample point have a higher sensitivity than that of T_{slope}. The results of bovine vertebra and ovine vertebra models are shown in Figs. 6(b) and 6(c). Similarly, it was found that F_{energy} has better distinction than T_{slope}. The values of T_{slope} have low sensitivity in distinguishing between the two different tissues, especially in the ovine vertebra experiment. In bovine vertebra experiment, the curve has large volatility.

4. Discussion

PS internal fixation has been commonly used for correcting instability of spine.[20] In PS fixation, there are two major problems to the effect of surgery outcomes. The first one is that the tip of traditional

instrument breaks the boundary of bone (cortical bone) and damages ambient tissues of patients. The second one is that the screw is not placed into the exact position and the fixation stability is not strong enough. The ideal position is that the screw is placed starting from the arch, through the cancellous bone and arrives at the cortical bone. In the previous study, the method using optical spectrum and needle-like probe based on the principle of local bone reflectance spectrum, provides a new way to overcome the two problems to the most extent.

In this study, various animal vertebra (porcine, bovine and ovine) were measured in the experiment. Although bovine and ovine vertebrae are different in structure from human vertebrae, they are similar in composition, used as vertebral models in some research.[12] We obtained different animal vertebra spectrum according to nine sampling points along the trajectory. In Fig. 2, each spectrum curve represents a specific sampling point on one animal vertebra. Points 1 and 9 are in the cortical bones and points 2 to 8 are in the cancellous bones. During different animal experiment, the values of points 1 and 9 were compared with those of points 2 to 8. We found that some values of points 1 and 9 were larger but some were not. It means the spectra of cancellous bones and cortical bones had similar shapes but with different values. The cause of this result is that different vertebra has different structures. It is the first time to search for the differences among spectra of different animal vertebra.

Frequency domain method was used to distinguish between cancellous bone and cortical bones. First, the spectra were divided into two groups based on the two tissues. Then, after the FFT of initial spectra, the average energy of the two groups from different bands were calculated and compared. A specific band (550 nm to 700 nm) was chosen because within it, the average energy showed the largest difference. Finally, based on this band we continued to obtain the average energy of frequency section. Since the information in frequency domain is usually more stable than that in time domain, thus F_{energy} (the average energy of 4 Hz to 5 Hz) is a better choice.

For method validation, we compared F_{energy} and T_{slope} according to different ways in this study. In Fig. 6, F_{energy} has better distinction between two different tissues in the three animal experiments. The results show that the values of F_{energy} on point 1 and 9 are both smaller than 2 and are much smaller than those on point 2 to 8 which are larger than 5. However, T_{slope} have low sensitivity in distinguishing between two different tissues and the values of T_{slope} on point 2 to 8 vary in a large range. In porcine vertebra experiment, the value of T_{slope} on point 4 is close to that on point 9, which indicates the distinction between two different tissues is small. Moreover, in bovine vertebra experiment, the curve of T_{slope} has larger volatility in cancellous bone than that of F_{energy}. Therefore, the sensitivity of using F_{energy} is higher than that of T_{slope}.

Near-infrared optical spectroscopy would not be the only way. Another optical spectroscopy has also been used in both clinical and basic science research about vertebra.[21,22] For example, the cartilage, subchondral bone and cancellous bone could be examined by fiber-optic Raman spectroscope and photoacoustic tomography.[23–25] As in other literature, the varying optical signal can provide some information about structures and composition of bone such as bone mineral crystallinity and tissue density. In this study, the cortical and cancellous bones are different in mineral crystallinity and density. We only provided one method in frequency domain such as the calculation of energy differences. The near-infrared optical spectrum will be characterized according to different domain in different animal experiment.

This paper provides real-time monitoring method during surgery. The distinguished pattern from spectrum can be used in surgery navigation. For the application, the pattern parameters must have high sensitivity. There are two things to be done to validate this method: first, the sample number needs to be increased and more calculation methods need to be improved and tested; second, the surgery requires much time and experienced surgeons. Bone research for other animal models should be done in further research, such as rabbit models.

5. Conclusion

In this project, an NIR optical fiber probe is employed to monitor the characteristic spectrum along the placement trajectory of PS in different animal vertebral bones. Based on it, we investigated the optical reflectance along the fixation trajectory of PS in frequency domain. The main research results of this study include: we measured the spectrum of vertebra tissue on the trajectory of pedicle screw. Fresh porcine vertebrae, bovine

vertebrae and ovine vertebrae were used in the experiments. F_{energy} and T_{slope} factors of vertebral bones and identifying model of pathway of PS were deduced. Sensitivity of the two patterns was evaluated and F_{energy} was proved to be the optimal identification factor. The results gained from this study are vital significant to the development of hi-tech medical instruments with independent intellectual property rights.

Conflict of Interest

No potential conflict of interest was reported by the authors.

Acknowledgments

This work was supported by the Nanjing Institute of Technology high level introduction of talents Research Fund (YKJ201862), the National Major Scientific Instruments and Equipment Development Project Funded by the National Natural Science Foundation of China (Grant Nos. 81827803 and 81727804), the National Natural Science Foundation of China (Grant Nos. 61703201, 61875085 and 81601532), Natural Science Foundation of Jiangsu Province (Grant Nos. BK20160814 and BK20170765).

References

1. K. Matsukawa, Y. Yato, R. A. Hynes, H. Imabayashi, N. Hosogane, T. Asazuma, T. Matsui, Y. Kobayashi, K. Nemoto, "Cortical bone trajectory for thoracic pedicle screws: A technical note," *Clin. Spine Surg.* **30**, 497–504 (2017).
2. P. Korovessis, E. Mpountogianni, V. Syrimpeis, A. Baikousis, V. Tsekouras, "Percutaneous injection of strontium containing hydroxyapatite versus polymethacrylate plus short-segment pedicle screw fixation for traumatic A2- and A3/AO-type fractures in adults," *Adv. Orthopedics* **2018**, 1–8 (2018).
3. I. Saarenpää, T. Laine, J. Hirvonen, S. Hurme, E. Kotilainen, J. Rinne, K. Korhonen, J. Frantzén, "Accuracy of 837 pedicle screw positions in degenerative lumbar spine with conventional open surgery evaluated by computed tomography," *Acta Neurochirurgica* **159**, 2011–2017 (2017).
4. I. D. Gelalis, N. K. Paschos, E. E. Pakos, A. N. Politis, C. M. Arnaoutoglou, A. C. Karageorgos, A. Ploumis, T. A. Xenakis, "Accuracy of pedicle screw placement: A systematic review of prospective in vivo studies comparing free hand, fluoroscopy guidance and navigation techniques," *Eur. Spine J.* **21**, 247–255 (2012).
5. F. Acosta, T. Thompson, S. Campbell, P. Weinstein, C. Ames, "Use of intraoperative isocentric C-arm 3D fluoroscopy for sextant percutaneous pedicle screw placement: Case report and review of the literature," *Spine J.* **5**, 339–343 (2005).
6. S. Rajasekaran, S. Vidyadhara, A. Shetty, "Intraoperative Iso-C3D navigation for pedicle screw instrumentation of hangman's fracture: A case report," *J. Orthopaedic Sur.* **15**, 73–77 (2007).
7. S. De Raedt, I. Mechlenburg, M. Stilling, L. Rømer, R. J. Murphy, M. Armand, J. Lepistö, M. de Bruijne, K. Søballe, "Reliability of computer-assisted periacetabular osteotomy using a minimally invasive approach," *Int. J. Comput. Assisted Radiol. Sur.* **13**, 2021–2028 (2018).
8. Q. Y. Wang, M. G. Huang, D. Q. Ou, Y. C. Xu, J. W. Dong, H. D. Yin, W. Chen, L. M. Rong, "One-stage extreme lateral interbody fusion and percutaneous pedicle screw fixation in lumbar spine tuberculosis," *J. Musculoskelet. Neuronal Interact* **17**, 450–455 (2017).
9. C. Bolger, M. Kelleher, L. McEvoy, M. Brayda-Bruno, A. Kaelin, J. Lazennec, H. Le, C. Logroscino, P. Mata, P. Moreta, G. Saillant, R. Zeller, "Electrical conductivity measurement: A new technique to detect iatrogenic initial pedicle perforation," *Eur Spine J.* **16**, 1919–1924 (2007).
10. Y. Liu, M. Kelleher, L. McEvoy, M. Brayda-Bruno, A. Kaelin, J. Lazennec, H. Le, C. Logroscino, Y. Wang, Z. Qian, J. Zhao, X. Cao, W. Li, "Monitoring the reduced scattering coefficient of bone tissues on the trajectory of pedicle screw placement using near-infrared spectroscopy," *J. Biomed Opt.* **19**, 1919–1924 (2014).
11. W. Li, Y. Liu, Z. Qian, "Determination of detection depth of optical probe in pedicle screw measurement device," *Biomed. Eng. Online* **13**, 148–163 (2014).
12. P. Huang, Y. Wang, J. Xu, B. Xiao, J. Liu, L. Che, K. Mao, "Minimally invasive unilateral pedicle screws and a translaminar facet screw fixation and interbody fusion for treatment of single-segment lower lumbar vertebral disease: Surgical technique and preliminary clinical results," *J. Orthopaedic Sur. Res.* **12**, 117 (2017).
13. F. E. Greene, S. Tauch, E. Webb, D. Amarasiriwardena, "Application of diffuse reflectance infrared fourier transform spectroscopy (DRIFTS) for the identification of potential diagenesis and crystallinity changes in teeth," *Microchem. J.* **76**, 141–149 (2004).
14. T. J. Farrell, M. S. Patterson, "A diffusion theory model of spatially resolved, steady-state diffuse

reflectance for the noninvasive determination of tissue optical properties in vivo," *Med. Phys.* **19**, 879–888 (1992).
15. R. A. Weersink, J. E. Hayward, K. R. Diamond, M. S. Patterson, "Accuracy of noninvasive in vivo measurements of photosensitizer uptake based on a diffusion model of reflectance spectroscopy," *Photochem. Photobiol.* **66**, 326–335 (1997).
16. B. M. Bass, "A low-power, high performance, 1024-point FFT processor," *IEEE J. Solid-Stage Circuits* **34**, 380–387 (1999).
17. L. R. Johnson, A. K. Jain, "An efficient two-dimensional FFT algorithm," *IEEE Trans. Pattern Anal. Mach. Intell.* **3**, 698–701 (1981).
18. C. Y. Lee, S. H. Chan, S. T. Lee, "A method to develop an in vitro osteoporosis model of porcine vertebrae: Histological and biomechanical study," *J. Neurosurg. Spine* **14**, 789–798 (2011).
19. F. F. Tamás, S. K. Frank, F. M. Anne, S. K. Zsolt, J. J. Dezső, "Prospective study of the effect of pedicle screw placement on development of the immature vertebra in an in vivo porcine mode," *Eur. Spine J.* **20**, 1892–1898 (2011).
20. J. I. Ryu, K. H. Bak, J. M. Kim, H. J. Chun, "Comparison of transarticular screw fixation and C1 lateral mass-C2 pedicle screw fixation in rheumatoid arthritis patients with atlantoaxial instability," *World Neurosur.* **99**, 179–185 (2017).
21. M. Uehara, J. Takahashi, S. Ikegami, S. Kuraishi, M. Shimizu, T. Futatsugi, H. Oba, M. Koseki, H. Kato, "Pedicle screw loosening after posterior spinal fusion for adolescent idiopathic scoliosis in upper and lower instrumented vertebrae having major perforation," *SPINE* **1**, 1895–1900 (2017).
22. G. Nayar, D. J. Blizzard, T. Y. Wang, S. Cook, A. G. Back, D. Vincent, I. O. Karikari, "Pedicle screw placement accuracy using ultra-low radiation imaging with image enhancement versus conventional fluoroscopy in minimally invasive transforaminal lumbar interbody fusion: An internally randomized controlled trial," *J. Neurosurg. Spine* **28**, 186–193 (2017).
23. W. Li, X. Sun, Y. Wang, G. Niu, X. Chen, Z. Qian, L. Nie, "In vivo quantitative photoacoustic microscopy of gold nanostar kinetics in mouse organs," *Biomed. Opt. Express* **5**, 2679–2685 (2014).
24. W. Li, R. Chen, J. Lv, H. Wang, Y. Liu, Y. Peng, Z. Qian, G. Fu, L. Nie, "In vivo photoacoustic imaging of brain injury and rehabilitation by high-efficient near-infrared dye labeled mesenchymal stem cells with enhanced brain barrier permeability," *Biomed. Opt. Express* **5**, 1–8 (2018).
25. L. Nie, X. Cai, K. Masiov, A. Garcia-Uribe, M. Anastasio, L. Wang, "Photoacoustic tomography through a whole adult human skull with a photon recycler," *J. Biomed. Opt.* **17**, 1–3 (2012).